Science of the Total Environment 650 (2019) 1371–1381

Contents lists available at ScienceDirect

Science of the Total Environment

journal homepage: www.elsevier.com/locate/scitotenv

Climate, forest growing season, and evapotranspiration changes in the central Appalachian Mountains, USA☆

Brandi A. Gaertner [a,*], Nicolas Zegre [b], Timothy Warner [c], Rodrigo Fernandez [b], Yaqian He [d], Eric R. Merriam [b]

[a] Health, Science, Technology, & Mathematics, Alderson Broaddus University, Philippi, WV 26416, United States of America
[b] Forestry & Natural Resources, West Virginia University, Morgantown, WV 26506, United States of America
[c] Geology & Geography, West Virginia University, Morgantown, WV 26505, United States of America
[d] Geography, Dartmouth College, Hanover, NH 04755, United States of America

HIGHLIGHTS

- Growing season length and evapotranspiration was assessed in the central Appalachian Mountains region
- Growing season length has increased by 22 days, while evapotranspiration increased by 12 mm
- The climatic variables temperature, vapor pressure deficit, wind, and humidity effect growing season length change
- A one day increase in growing season length is partially responsible for increasing evapotranspiration by 0.5 mm
- The results of this study are important for runoff and evapotranspiration prediction modelling and forest water management

GRAPHICAL ABSTRACT

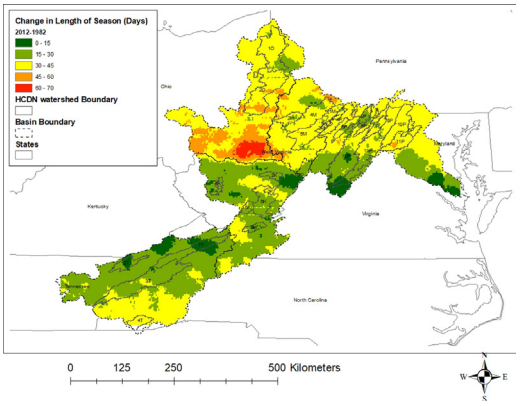

ARTICLE INFO

Article history:
Received 17 April 2018
Received in revised form 7 September 2018
Accepted 9 September 2018
Available online 12 September 2018

Editor: R Ludwig

Keywords:
Growing season length
Evapotranspiration
Humidity
Water cycle
Climate change
Temperate forests

ABSTRACT

We analyzed trends in climatologic, hydrologic, and growing season length variables, identified the important variables effecting growing season length changes, and evaluated the influence of a lengthened growing season on increasing evapotranspiration trends for the central Appalachian Mountains region of the United States. We generated three growing season length variables using remotely sensed GIMMS NDVI3g data, two variables from measured streamflow, and 13 climate parameters from gridded datasets. We included various climate, hydrology, and phenology explanatory variables in two applications of Principle Components Analysis to reduce dimensionality, then utilized the final variables in two Linear Mixed Effects models to evaluate the role of climate on growing season length and evapotranspiration. The results showed that growing season length has increased, on average, by ~22 days and evapotranspiration has increased up to ~12 mm throughout the region. The results also suggest that a suite of climatic variables including temperature, vapor pressure deficit, wind, and humidity are important in growing season length change. The climatic variables work synergistically to produce greater evaporative demand and atmospheric humidity, which is theoretically consistent with intensification of the water cycle and the Clausius-Clapeyron relation, which states that humidity increases nonlinearly by 7%/K. Optimization of the evapotranspiration model was increased by the inclusion of growing season length, suggesting that growing season length is partially responsible for variations in evapotranspiration over time. The results of this research imply that a longer growing season has the potential to increase forest water cycling and

☆ This draft manuscript is distributed solely for the purposes of scientific peer review. Its content is deliberative and pre-decisional, so it must not be disclosed or released by reviewers.

* Corresponding author.
E-mail address: bagaertner@mix.wvu.edu (B.A. Gaertner).

https://doi.org/10.1016/j.scitotenv.2018.09.129

evaporative loss in temperate forests, which may lead to decreased freshwater provisioning from forests to downstream population centers. Additionally, results from this study provide important information for runoff and evapotranspiration modelling and forest water management under changing climate.

1. Introduction

Forests play a critical role in provisioning freshwater resources to downstream regions (Viviroli and Weingartner, 2004) but climate change has affected growing season length (Schwartz et al., 2002), having implications for the terrestrial water cycle (Creed et al., 2015; Hwang et al., 2014). Therefore, it is critical to understand how forest growing season change alters rainfall partitioning into evaporation and runoff in deciduous forests, in order to sustainably manage forested headwater watersheds as a source of freshwater. Higher air temperatures have resulted in greater fluxes of precipitation (P) and evapotranspiration (ET) between the terrestrial and atmospheric systems, leading to water cycle intensification (Huntington, 2010; Trenberth et al., 2007). Growing season length partially controls ET, which cycles up to 62% of terrestrial water to the atmosphere (Dingman, 2015). P and atmospheric evaporative demand have increased due to warmer temperatures (Huntington, 2010; Trenberth et al., 2007), leading to changing annual water yields (Campbell et al., 2011; Jones et al., 2012; Wang and Hejazi, 2011), with humid regions tending to become wetter while arid regions have tended to become drier (Chou et al., 2009). A longer growing season has the potential to alter water cycle fluxes through increased plant water use and ET (Hwang et al., 2014) in deciduous forests, which can potentially alter forest freshwater partitioning into streamflow (Q) and ET (Creed et al., 2015). Understanding these interactions is vital for future Q and ET projections as well as for sustainably managing headwater forests.

Intensification of the water cycle is theoretically consistent with the Clausius-Clapeyron relation (Held and Soden, 2000), which states that warmer air holds more water (e.g. greater maximum specific humidity) and that consequently, atmospheric water vapor tends to increase nonlinearly with increases in air temperature. A warmer climate can also increase growing season length and provide more energy for ET, potentially decreasing Q (Hwang et al., 2014). Studies have shown that over recent decades growing season has arrived earlier in general in temperate forests (Chmielewski and Rötzer, 2001; Creed et al., 2015; Jeong et al., 2011; Lebourgeois et al., 2010; Richardson et al., 2006; Schwartz et al., 2006). Warmer air temperature has been identified as an important climate variable for growing season length changes (Dragoni and Rahman, 2012; Morin et al., 2010) but recent studies have found that temperature (Marchin et al., 2015; Wolkovich et al., 2012) and photoperiod (Bauerle et al., 2012) alone do not explain phenological variations in temperate forests. The water cycle itself could potentially impact the growing season through increased rate of humidity, which have been shown to signal spring onset and fall senescence in forests (Hu et al., 2011; Laube et al., 2014).

In the densely populated eastern USA, the heavily forested mountains of central Appalachian Mountains play a critical role in freshwater provisioning, providing approximately 30% (Caldwell et al., 2014) of water used by downstream communities (Caldwell et al., 2016; Parker et al., 1907). The central Appalachian Mountains region encompasses West Virginia (WV), parts of Virginia (VA), North Carolina (NC), Maryland (MD), and Tennessee (TN) (ARC, 1970). This region is >80% forested (Slayer, 2014), has steep slopes, and geographic variability that includes high elevation and coastal areas. As a regional water source (Viviroli et al., 2007) for approximately 9% of the U.S. population (U.S._Census_Bureau, 2009), the central Appalachian Mountains region is representative of other temperate forests that provide freshwater services around the globe. Climate driven shifts in freshwater partitioning in forests could impact water supplies for major population centers downstream.

The overall objective of this paper is therefore to quantify long-term changes in climate, water balance components, and growing season length across the region to provide insight into the interactions between climate change, growing season length, and ET. We hypothesize that humidity is an important climatic variable of growing season length changes and that a lengthened growing season is in part responsible changing evapotranspiration. In testing this hypothesis, the following questions are explored:

1. How has historical climate, growing season length, and water balance components changed over time throughout the central Appalachian Mountains region?
2. What are the climatic variables important to growing season length changes in the temperate forests of the region?
3. How do changes in growing season length effect forest ET throughout the region?

2. Study area

Our study area consists of 31 watersheds located across five dominant river basins that collectively cover 125,000 km^2 in the eastern USA (Fig. 1). Of the five basins, 4 (Monongahela, Upper Ohio, Kanawha, and Tennessee) drain west to the Mississippi River and Gulf of Mexico, while the Potomac River drains east to Washington D.C. and the Chesapeake Bay. The 31 watersheds selected for this study are part the U.S. Geological Survey Hydro-Climatic Data Network (HCDN) (Slack and Landwehr, 1992). HCDN consists of streamflow station data for minimally impacted (<10% human influence such as reservoirs, diversion, land use change, or severe ground-water pumping) watersheds. A regional land cover analysis using data from the 2011 National Land Cover Database (NLCD) (Homer et al., 2015) was used to verify that watersheds met the HCDN definition (Fig. 2). The HCDN watersheds selected for this research cover approximately 39% of the total area in the five river basins, with seven watersheds in the Kanawha basin, five watersheds in the Monongahela basin, two watersheds in the Ohio basin, thirteen watersheds in the Potomac Basin, and four watersheds in the Tennessee basin. The forests are mostly classified as mixed mesophytic, dominated by hardwood species (e.g. *Quercus* (oaks), *Betula* (birch), *Fagus* (birch), *Acer* (maple), *Populus* (poplar)) located on ridges and hillslopes, and coniferous (*Pinus* (pine), *Tsuga* (hemlock)) at higher elevations and along stream networks (Day et al., 1988; Slayer, 2014).

The region's climate is characterized as humid marine in the eastern/Atlantic coastal area and humid continental on the western edge (Konrad

Fig. 1. A. Location of the study region in the central Appalachian Mountains region of the eastern USA. B. Study Area depicting the conceptual change in growing season length from 1982 and 2012 (e.g. LOS in 2012 – LOS in 1982). Green regions represent minimal change between the two years (0–15 days) while red represents maximum change (60–70 days). The dashed lines depict basin boundaries Potomac (P), Monongahela (M), Ohio (O), Kanawha (K), and Tennessee (T). The solid lines outline the 31 watersheds, and the identifiers label the basin followed by an HCDN (Slack and Landwehr, 1992) watershed number from 1 to n.

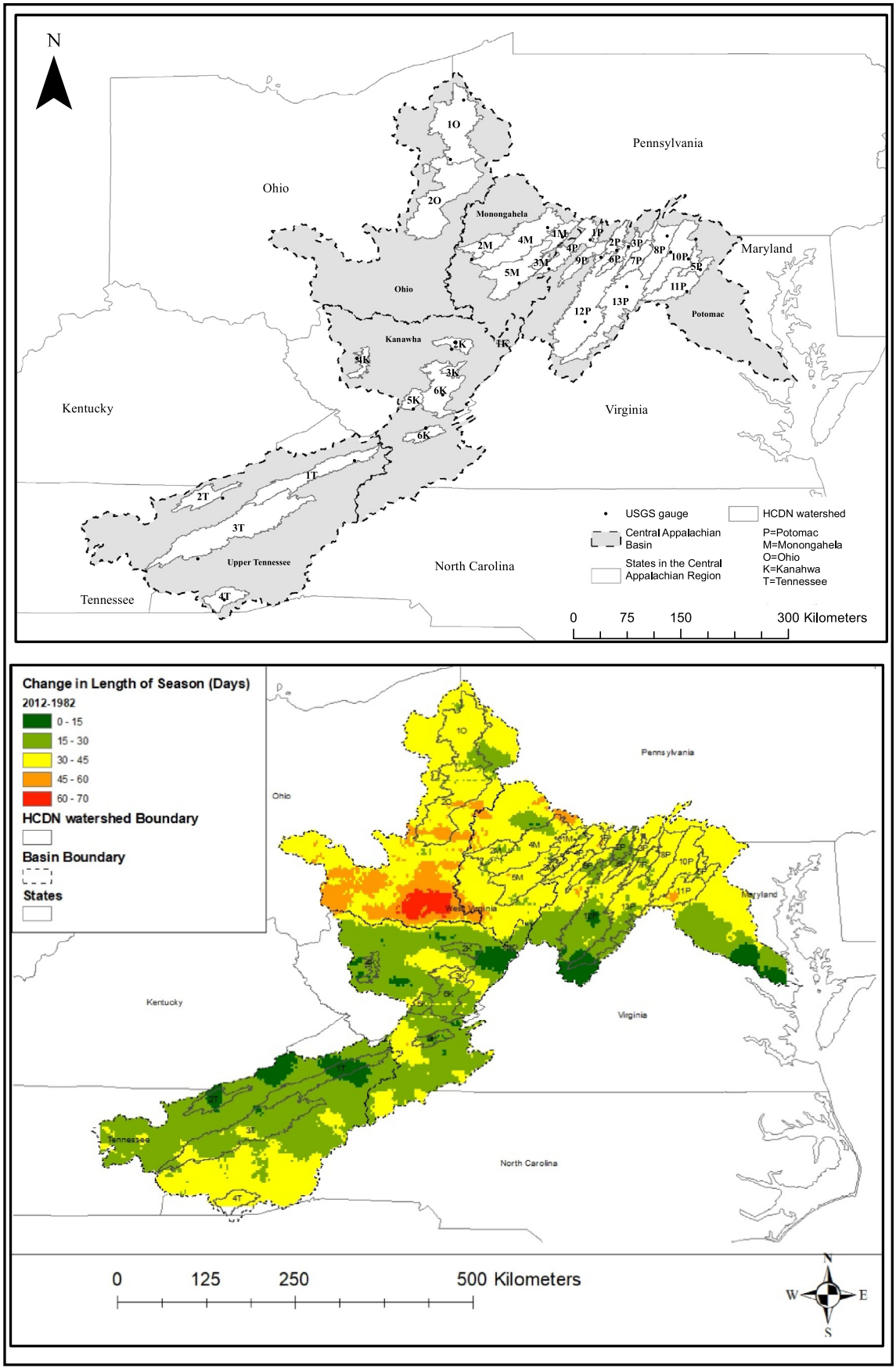
N
Pennsylvania
Ohio
Maryland
Kentucky
Virginia
North Carolina
Tennessee
Monongahela
Ohio
Kanawha
Potomac
Upper Tennessee
1O
2O
1M
2M
3M
4M
5M
1P
2P
3P
4P
5P
6P
7P
8P
9P
10P
11P
12P
13P
1K
2K
3K
4K
5K
6K
1T
2T
3T
4T
USGS gauge
Central Appalachian Basin
States in the Central Appalachian Region
HCDN watershed
P=Potomac
M=Monongahela
O=Ohio
K=Kanawha
T=Tennessee
0 75 150 300 Kilometers
Change in Length of Season (Days)
2012-1982
0 - 15
15 - 30
30 - 45
45 - 60
60 - 70
HCDN watershed Boundary
Basin Boundary
States
0 125 250 500 Kilometers
W
E
S

and Fuhrmann, 2013). Mean annual temperature ranges from 9.3 °C in the mountains to 14.7 °C near the ocean, and increases with decreasing latitude, with the northernmost Ohio River basin averaging 10.5 °C, and the southernmost Tennessee River basin averaging 15 °C. P is relatively evenly distributed throughout the year, dominated by small, low intensity storms with intermittent high intensity frontal thunderstorm events (Keim, 1996; Keim, 1997; Konrad and Fuhrmann, 2013). Annual P increases with elevation from 1034 mm in the Potomac River basin to 1870 mm in the Tennessee River basin. Average annual ET loss is ~75% of annual rainfall in all watersheds except the Monongahela, the most heavily forested basin, which averages ~51% of P (Adams et al., 2012; Farnsworth and Thompson, 1983; Ford et al., 2005; Harstine, 1991; Miller and Weaver, 1971).

3. Methods

3.1. Data

3.1.1. Vegetation phenology from satellite imagery

For this study, we extracted long term phenological records from the Global Inventory Modeling and Mapping Studies (GIMMS) third generation Normalized Difference Vegetation Index (NDVI3g) to characterize the temporal trends in regional scale phenology (Hong and Zhang, 2006; Prebyl, 2012). NDVI3g is produced from data acquired by the Advanced Very High Resolution Radiometer (AVHRR) on board the National Oceanic and Atmospheric Administration (NOAA) satellite series (Pinzon and Tucker, 2014). NDVI data were extracted from October 1982 to September 2012 to quantify recent changes in growing season length throughout the region.

Data were quality-controlled based on data reliability where pixels with weak or noisy time series (e.g. quality flag > 3), NDVI values that were negative, equal to zero, or >1.0, high outlier values, or Julian day > 365, were removed for the analysis. The TIMESAT program (Jönsson and Eklundh, 2004) was used to produce a smoothed NDVI time series dataset from 1982 to 2012. TIMESAT incorporates an automated median-spike pre-processing technique to remove spikes and outliers (Vidal and Amigo, 2012). The Asymmetric Gaussian function was used to fit a smooth continuous curve to extract phenological signals from the data (Fig. 3). NDVI values between 0.8 and 1.0 that represent dense forested land-cover were selected for this analysis. Data output were in annual time series sets (e.g. 31 years per derived phenological attribute per pixel). Start of season (SOS) and end of season (EOS) were estimated as the date where NDVI increased or decreased to 50% of the amplitude, representing canopy development and senescence respectively, and length of season (LOS) was calculated as end of season minus the SOS (Fig. 3) (White et al., 1999; White et al., 2009).

3.1.2. Hydrologic variables

Mean annual streamflow data for the 31 HCDN watersheds were obtained from the USGS historical water dataset (http://waterdata.usgs.gov) using R (Hirsch and De Cicco, 2015; RCore, 2013). Streamflow data were then normalized by area, and averaged annually to produce mean annual *Q*.

Actual ET in mm/year was estimated using the annual water balance, assuming no change in storage

$$ET = P - Q + \Delta S$$

where P is P, Q is average Q, and ΔS is watershed storage (e.g. groundwater, soil moisture, vegetation/root) which approaches zero on an annual scale, all in mm/year.

3.1.3. Climate variables

Annual maximum and minimum vapor pressure deficit and dew pressure temperature data were extracted from PRISM (Parameter Elevation Regression on Independent Slopes) (Daly et al., 1997). PRISM uses 13,000 P and 10,000 surface temperature data stations over the conterminous US to spatially interpolate P and temperature using a Digital Elevation Model (DEM) to estimate orographic effects. PRISM is gridded at a 4 km spatial resolution at the daily time scale, and covers the period from 1895 to the present (Daly et al., 2008).

Ten annual climate variables (maximum and minimum temperature, P, potential ET, maximum and minimum relative humidity, solar radiation, wind direction, wind speed, specific humidity) were extracted from the gridded (4 km spatial resolution) MetData meteorological dataset (Table 1) (Abatzoglou and Brown, 2012). MetData was developed by combining the hourly and 1/8th degree resolution North America Land Data Assimilation System Phase 2 (NLDAS-2) dataset with the monthly 4 km resolution PRISM dataset from 1979 to 2015 (see Abatzoglou and Brown (2012)). Potential ET was calculated using the Penman-Monteith equation (Penman, 1948) forced with solar radiation, dew point temperature, wind speed, and evaporation. Wind direction was normalized to account for the 0–360-degree direction. Using wind speed and wind direction angle, we calculated the *x* and *y* components using trigonometric functions (Breckling, 2012). All daily variables predicting growing season were aggregated to US annual water year (October 1 – September 31). However, all variables used to predict evapotranspiration were conducted using the vegetation year (May–April) (Troch et al., 2009) using R (RCore, 2013). Vegetation year minimizes the delta storage term in estimating evapotranspiration from precipitation by accounting for soil moisture depletion from a longer growing season the current year and the subsequent altered stream discharge patterns the following dormant season. This is especially effective in estimating ET given the central Appalachian region does not have dominant snowpack (Troch et al., 2009).

3.2. Statistical methods

3.2.1. Quantifying trends in climate and growing season length

The rank-based, non-parametric Mann Kendall statistical test was used to detect trends in climate, hydrology, and growing season variables (Helsel and Hirsch, 1992). Mann Kendall allows for non-normally distributed data (Andreadis and Lettenmaier, 2006) and allows for missing values (Hirsch and Slack, 1984) and is commonly used for detecting trends in hydrology and hydro-meteorological studies (Yue et al., 2002). Trends were considered significant at the $\alpha = 0.05$ level. The direction and magnitude of the time series trends were estimated using the Kendall Thiel Sen slope, which identifies the median slope among all lines through a time series (Helsel and Hirsch, 1992). Total change over the 31-year study period was estimated by multiplying slope by the number of years of data (i.e. 31 years) (Zegre et al., 2014).

3.2.2. Identifying important components of growing season length change

3.2.2.1. Principle component analysis. Given the large number of potential explanatory variables that drive growing season length, a principle components analysis (PCA) (Bibby et al., 1979) was used to reduce the dimensionality of the variables. The original dataset included 14 predictor variables: thirteen climate variables (P, specific humidity [sph], average annual minimum [rmin] and maximum relative humidity [rmax], solar radiation [srad], dew pressure temperature [dpt], average annual minimum [tmin] and maximum temperature [tmax], potential evapotranspiration [PET], wind direction [th], and wind speed [vs], maximum [vpdmax] and minimum vapor pressure deficit [vpdmin], and one hydrology variables (Q)). The input data represented a three-dimensional matrix, comprising the climate/hydrology as the variables in one dimension, with time and space as the remaining two dimensions, yielding ~14,000 observations (31 years * 31 sites) for each of the 15 variables. Standardized principle component analysis was implemented using R. Principle components with eigenvalues >1.0 were regarded as carrying important information, and factor loadings

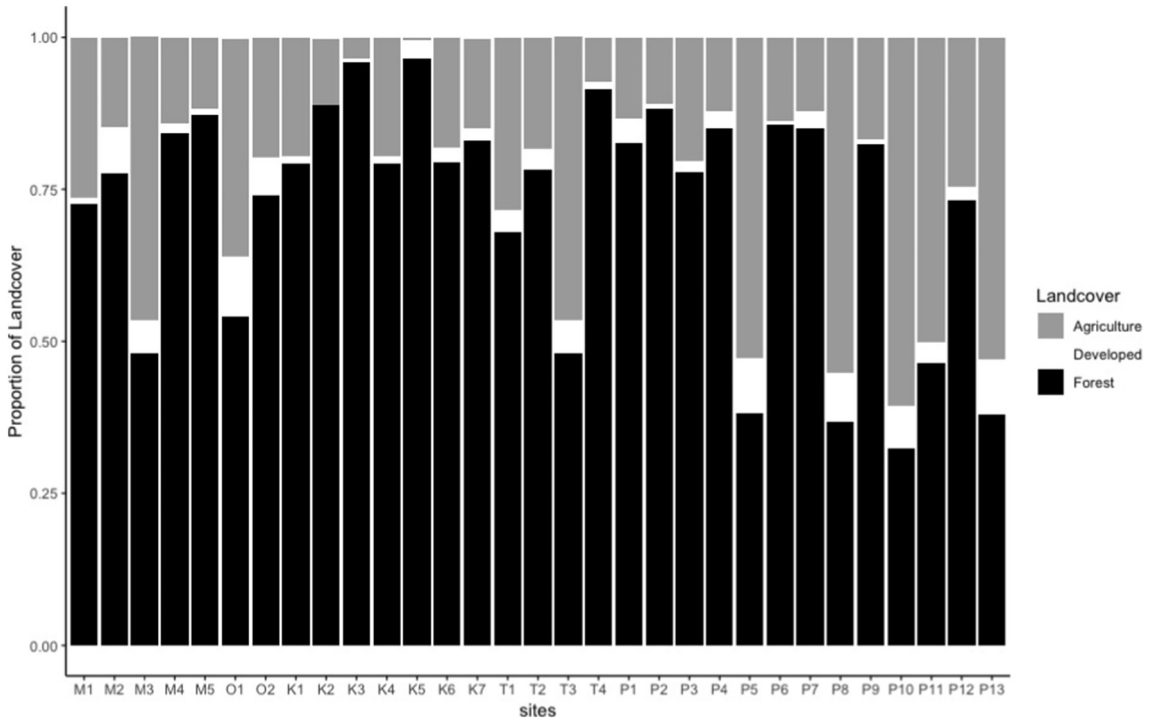

Fig. 2. Land Cover composition depicting proportion agriculture, developed, and forest for the 31 watersheds based on 2011 NLCD land cover analysis throughout the central Appalachian region. Forests include deciduous, evergreen, and mixed forests, developed includes open space, barren land, low, medium, and high intensity development, and agriculture includes herbaceous, hay/pasture, and cultivated crops.

rounding to an absolute value ≥0.4 were considered important in determining a particular component (McCune et al., 2002).

A correlation matrix between climate and hydrologic variables was developed to remove statistically redundant variables. A Pearson correlation matrix was developed using R (RCore, 2013). All correlation values >0.7 were considered strongly related (e.g. r > ±0.7) (Ratner, 2009).

3.2.2.2. Mixed effects model. A linear mixed effects model (Zuur et al., 2009) was developed to identify the important climatic variables in growing season length using the explanatory variables identified by the PCA. A linear mixed effects model is a statistical correlation model used to identify interactions between variables in a longitudinal study, with applicability in multiple disciplines including physical, biology, and social sciences. Linear mixed effects models contain fixed and random components (Zuur et al., 2009), which allows for spatial and temporal variability in site-specific topography, climate, geography, and time. We validated our model by randomly splitting data into training (80%, n = 11,532) and test (20%, n = 2884) data. The model was developed by iteratively dropping fixed and random parameters (Arnold, 2010). All dropped parameters that increased the Akaike Information Criteria (AIC) value >2 were removed to develop the final model (Arnold, 2010). Model performance was evaluated using the AIC values, root mean square error, marginal coefficient of determination, which is the variance explained by fixed effects, and conditional coefficient of determination, which is the variance explained by fixed and random effects together (collectively R^2) using R (Bartoń, 2013; RCore, 2014).

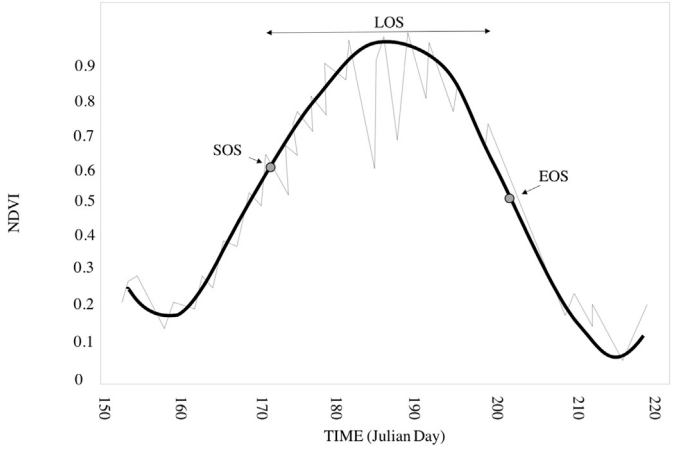

Fig. 3. Figure depicting the process for extracting phenology variables from time series of NDVI data using the program TIMESAT. Gray lines represent NDVI data, the black line represents the smoothed timesat vegetation signal, the gray dots represent 50% canopy at start (SOS) and end of season (EOS), LOS represents the difference between EOS and SOS.

Table 1
Summary table for all variables and acronyms.

Variable	Acronym
Precipitation	P
Evapotranspiration	ET
Specific humidity	sph
Average annual maximum temperature	tmax
Average annual minimum temperature	tmin
Average annual maximum humidity	rmax
Average annual minimum relative humidity	rmin
Solar radiation	srad
Dew pressure temperature	DPT
Potential evapotranspiration	PET
Wind direction	th
Wind speed	vs
Maximum vapor pressure deficit	vpdmax
Minimum vapor pressure deficit	vpdmin
Runoff	Q
Start of season	SOS
End of season	EOS
Length of season	LOS

3.2.3. Interaction of growing season length and evapotranspiration change

3.2.3.1. Principle component analysis. To reduce the dimensionality of the potential explanatory variables important to ET, a PCA was conducted on 17 climatic variables. The PCA included three growing season variables (start of season [SOS], end of season [EOS], length of season [LOS]), thirteen climate variables (P, specific humidity [sph], average annual minimum [rmin] and maximum relative humidity [rmax], solar radiation [srad], dew pressure temperature [dpt], average annual minimum [tmin] and maximum temperature [tmax], potential evapotranspiration [PET], wind direction [th], and wind speed [vs], maximum [vpdmax] and minimum vapor pressure deficit [vpdmin], and one hydrology variable (Q)).

The input data represented a three-dimensional matrix, comprising the climate/phenology as the variables in one dimension, with time and space as the remaining two dimensions, yielding ~18,000 observations (31 years * 31 sites) for each of the 17 variables. A correlation matrix between growing season, climate, and hydrologic variables was developed to remove statistically redundant variables.

To identify if growing season influences ET, a second mixed effects model was developed using the important variables identified by the PCA as fixed effects and site and year as random effects. The final model was similarly developed by iteratively dropping variables that increased the AIC value > 2. Model performance was evaluated using the AIC values, root mean square error, marginal coefficient of determination, and conditional coefficient of determination. The model was validated by randomly splitting data into training (80%, n = 14,607) and test (20%, n = 3651) data.

4. Results

4.1. Question 1: how has climate and growing season length changed?

4.1.1. Climate

Measured air temperatures generally increased across the watersheds over the 31 years studied. Maximum temperatures averaged 17.3 °C across the watersheds, and although most individual watersheds indicated warming temperatures, trends were not significant at $\alpha = 0.05$ for any watersheds (Table 2). Minimum temperatures increased significantly in 14 individual watersheds, increasing on average, by 0.2 °C. Solar radiation, which averaged 172.0 mW m^{-2} across all watersheds increased significantly in 10 watersheds by an average of 5.7 mW m^{-2} on average (SI Table 3). Potential evapotranspiration, which averaged 1076.0 mm across all watersheds, increased significantly by 64.9 mm in only one watershed. Minimum vapor pressure deficit, which averaged 0.72 hPa across watersheds, significantly decreased by −0.008 hPA in 17 watersheds (SI Table 3). Maximum vapor pressure deficit, which averaged 12.09 hPa across watersheds, significantly increased by 0.05 hPa at one watershed. Specific humidity, which averaged 0.7 g/kg across watersheds, significantly increased by 0.6 g/kg at one watershed (SI Table 3). Similarly, maximum relative humidity, which averaged 89%, significantly decreased by 2.2% on average, at eight watersheds (Table 2).

Wind, which is an important component of ET, also has increased across watersheds. Over the 31-year period studied, the average wind direction, calculated as degrees from north, was 254°, and has shifted 16° counter-clockwise to 238° in all watersheds, suggesting an increased northwesterly component (Table 2). Wind speed, which

Table 2
Mann Kendal trend table and total change over 31 years for the 31 watersheds in the central Appalachian region. Watershed Identifiers represents each watershed within the five basins, shown in Fig. 1. Station number and station name refer to USGS stream gauge identifiers. Bold represents significance at the 0.05 level and bold + italics represents significance at the 0.01 level.[a]

Watershed identifier	tmax (°C)	sph (g/kg)	rmax (%)	srad (mW/m^2)	LOS[b] (days)	th (°clock-wise from north)	vs (m/s)	ET (mm)	vpdmin (hPa)
1M	0.04	0.08	**−2.37**	1.41	***24.31***	***6.72***	0.078	7.66	***−0.008***
2M	0.11	0.02	**−2.55**	1.61	***23.17***	***8.84***	0.097	27.60	0.002
3M	−0.02	0.17	0.34	1.83	***28.18***	***6.51***	**0.101**	***32.52***	**−0.007**
4M	0.12	0.04	**−2.47**	1.48	***28.18***	***7.90***	**0.099**	2.02	−0.004
5M	0.08	0.11	−1.33	1.78	***31.14***	***7.53***	0.085	***19.88***	−0.004
1O	0.11	0.29	−1.65	**4.45**	***22.58***	***12.64***	0.098	−2.01	**−0.011**
2O	0.16	0.25	**−1.83**	3.30	***23.94***	***5.73***	**0.126**	9.62	**−0.009**
1K	−0.12	0.08	***−1.80***	1.06	5.47	***14.29***	**0.109**	3.43	**0.001**
2K	−0.27	0.09	***−1.91***	0.71	***16.74***	***14.36***	***0.112***	***31.20***	0.000
3K	−0.31	−0.13	−2.30	1.03	***25.36***	***17.98***	***0.156***	6.21	0.001
4K	0.24	0.29	−0.26	3.26	***24.55***	***13.82***	**0.097**	**17.94**	**−0.007**
5K	0.29	0.16	−1.37	0.39	***24.20***	***20.38***	***0.151***	**17.83**	0.005
6K	0.02	−0.03	**−2.00**	0.61	***19.45***	***19.79***	***0.146***	***14.39***	0.001
7K	0.19	0.19	1.56	0.77	***19.73***	***23.81***	***0.171***	11.46	−0.002
1T	0.05	**0.57**	1.75	4.55	***17.28***	***14.46***	0.099	**15.27**	−0.004
2T	0.36	0.30	−1.21	***7.36***	***11.67***	***13.94***	0.052	**18.33**	***0.011***
3T	0.42	0.30	−0.88	**6.25**	***16.68***	***13.01***	0.074	42.07	0.000
4T	0.23	0.25	−1.52	**3.96**	***13.56***	***37.47***	0.043	−5.99	***0.010***
1P	0.27	0.01	**−2.46**	2.91	***24.80***	***17.71***	***0.147***	***30.32***	***−0.012***
2P	0.18	0.07	−1.85	3.95	***23.67***	***15.96***	***0.149***	15.22	**−0.011**
3P	0.25	0.20	−0.95	**4.84**	***25.83***	***20.76***	***0.170***	8.00	−0.004
4P	0.08	0.08	−1.95	2.18	***28.22***	***10.84***	**0.098**	12.36	***−0.013***
5P	0.10	0.22	−0.74	***6.91***	***17.27***	***19.97***	***0.169***	5.88	***−0.022***
6P	0.13	0.10	−1.41	4.04	***26.57***	***17.69***	***0.133***	5.83	***−0.011***
7P	0.27	0.27	−0.44	**4.78**	***24.58***	***19.80***	***0.146***	−2.49	−0.007
8P	0.40	0.28	−0.77	**5.95**	***26.76***	***18.21***	***0.170***	8.66	−0.002
9P	0.06	0.07	−1.39	3.19	***23.58***	***14.08***	***0.137***	8.66	***−0.014***
10P	0.36	0.21	−0.57	***6.32***	***24.06***	***18.18***	***0.163***	11.62	***−0.012***
11P	0.17	0.20	−0.88	**6.25**	***15.19***	***28.95***	***0.168***	8.37	***−0.016***
12P	N/A	0.08	−0.64	3.24	***17.17***	***12.05***	0.056	3.21	***−0.013***
13P	0.03	0.16	−1.79	4.03	***18.53***	***14.06***	0.040	9.48	−0.007
Average	0.1	0.2	−1.2	3.4	21.7	15.72	0.12	12.7	−0.005
Significant average	NA	**0.6**	**−2.18**	**5.7**	**22.2**	**15.72**	**0.15**	**22.0**	**−0.008**

[a] Table only includes variables included in later analysis.
[b] Length of growing season (LOS) calculated as SOS-EOS, at 50% canopy.

averaged 1.2 m/s across all watersheds, significantly increased at 21 watersheds by an average of 0.15 m/s (Table 2).

4.1.2. Hydrology

Water balance variables, including P, ET, and Q, also provide some evidence of change over the 31 years studied. P, which averaged 1126 mm across watersheds, increased in all but four watersheds by an average of 34 mm, although the change was not significant. Q averaged 512.0 mm across watersheds, and similar to P, changes were not significant at any individual watershed (SI Table 3). Although P and Q changes were not significant, variability tends to be minimized in water balance calculations, and thus ET potentially provides a more reliable record (Koster and Suarez, 1999; Sankarasubramanian and Vogel, 2002). Hence, ET was used, instead of Q as a response variable because it eliminates monthly variability given its dependency on available energy rather than P events thereby providing a more stable water response variable (Coopersmith et al., 2012; Fernandez and Sayama, 2015). ET, which averaged 613.0 mm across watersheds, increased in 28 watersheds, nine of which were significant. Across the entire region ET increased by 12.7 mm on average, for the statistically significant watersheds the increase was 22 mm (Table 2).

4.1.3. Growing season length

The results of the Mann Kendall trend analysis for growing season length indicated that SOS and EOS have changed significantly ($\alpha = 0.05$) across the region. SOS has advanced (i.e. spring is earlier) significantly in 25 watersheds by an average of 16.3 days. EOS has retreated (i.e. senescence is later in the year) by an average of 10.7 days and was significant at all watersheds (SI Table 3). The LOS, which averaged 179 days, increased significantly in 30 of the 31 sites, by an average of 22.2 days (Table 2).

Growing season length increases, as shown in the map of growing season changes from 1982 to 2012 (e.g. LOS 2012-LOS 1982) (Fig. 1b) were greatest in the southern extent of the Ohio river basin, increasing by as much as 70 days in some areas. Watersheds in the Kanawha and northern Tennessee basins increased the least, with changes that ranged from 0 to 15 days in some areas (Fig. 1b).

4.2. Question 2: what are the predictors of growing season length?

The first PCA analysis focused on the climate variables that potentially could be used in the mixed effect model for predicting growing season length, and the results were used to guide variable selection for the model. Four growing season length components were significant. Component 1, which explained 43% of the variance was characterized by an energy signature; component 2, which explained 25% of the variance, was characterized by a moisture availability signature; component 3, which explained 8.5% of the variance, consisted of evaporative turbulence signature; and component 4, which explained 6.5% of the variance, consisted of an evaporative demand signature (SI Table 4). Maximum temperature was correlated with dew pressure temperature ($R^2 = 0.82$), potential evapotranspiration (0.85), and minimum temperature ($R^2 = 0.87$) therefore, potential evapotranspiration, dew pressure temperature, and minimum temperature were eliminated from the model since maximum temperature had a higher factor loading.

The PCA analysis identified eight variables that were potentially important inputs for the mixed effect model: maximum temperature, specific humidity, relative humidity, wind direction, wind speed, precipitation, solar radiation, and minimum vapor pressure deficit as fixed effects. The optimal effect structure included random intercepts and slopes around year and site (SI Table 4).

The final model of growing season length showed significant fixed effects at alpha = 0.05 for maximum temperature (p-value = 0.008), minimum vapor pressure deficit (p-value = 0.034), wind direction (p-value = 0.024), and wind speed (p-value = 0.02). Significant interactive effects included maximum relative humidity and specific humidity (p-value = 0.024), maximum temperature and vapor pressure deficit (p-value = 0.04), and vapor pressure deficit with wind speed (p-value: 0.017) (SI Table 5). Together, fixed and random effects explained 88.3% of total variance in growing season length with a conditional $R^2 = 0.88$. Fixed effects explained 7.7% of the overall variation with a marginal $R^2 = 0.077$. When predicting growing season changes with the evaluation dataset, the final model had an overall root mean square error and uncertainty value of ±3.4 days.

4.3. Question 3: does growing season length influence evapotranspiration?

The second PCA analysis focused on the variables that could potentially be used to identify ET controls. Four significant principle components were identified for ET. Component 1, which explained 35% of the variance, was characterized by an energy signature. Component 2 (20%), was characterized by a moisture availability signature. Component 3 (11%), was characterized by a growing season signature. Component 4 (8%) was characterized by an evaporative demand signature (SI Table 6).

Thus, the variables included in the mixed effect model were maximum temperature, specific humidity, relative humidity, LOS, wind speed and wind direction, as well as the random effects of year and site. The list excluded potential evapotranspiration because it was significantly correlated with maximum temperature, and the latter had a higher loading in the PCA. Similarly, SOS and EOS were also eliminated from the model, since these variables were significantly correlated with LOS, which had the highest loading (0.59) of the three variables.

The final mixed effects model identified relative humidity as a significant predictor of ET at alpha = 0.1 (p-value = 0.059, respectively). LOS was not a significant individual variable but the interaction of LOS with maximum temperature, maximum relative humidity, specific humidity, wind speed, wind direction, and solar radiation resulted in a more optimal model (SI Table 7). Together, fixed and random effects explained 85% of the total variance in ET (conditional $R^2 = 0.846$). Fixed effects explained 0.8% of the total variance (marginal $R^2 = 0.0081$). The final model had an overall root mean square error of 87.2 mm when predicting ET with evaluation data.

5. Discussion

5.1. Question 1: how has climate and growing season length changed?

Previous studies have shown that air temperatures in the mid- and south-Atlantic region of the US that includes the central Appalachian region have increased between 0.5 and 1.9 °C, on average (Patterson et al., 2012; Pitchford et al., 2011). Higher air temperature increases the capacity of the atmosphere to hold water, theoretically leading to intensification of the hydrologic cycle in the form of accelerated rates of ET and P (Huntington, 2010; Trenberth et al., 2007). Greater rates of ET occur in response to increasing atmospheric and evaporative demand including vapor pressure deficit, wind turbulence, and rainfall inputs. These ideas are summarized by the Clausius-Clapeyron relation (Fig. 4), which states that with increasing temperatures, atmospheric water vapor exponentially increases by between 3.4%/K (Allen and Ingram, 2002) and 7%/K (Held and Soden, 2000), although there is debate about whether the water vapor increases associated with climate warming follows the higher or lower rate (Allen and Ingram, 2002). Our results are theoretically consistent with the Clausius-Clapeyron relation, albeit at the lower slope ($4.095e^{0.03x}$), equivalent to 3.4%/K rather than 7%/K that has a slope of $2.56e^{0.06x}$ (Fig. 4).

Increasing temperatures and water availability for tree growth over the study period from 1982 to 2012 have resulted in a lengthened growing season by ~22 days on average throughout the central Appalachian Mountains region. Greater change was observed in the spring (16 days) than the change during the senescence in the fall (10 days). Regional and local trends documented in previous studies corroborate

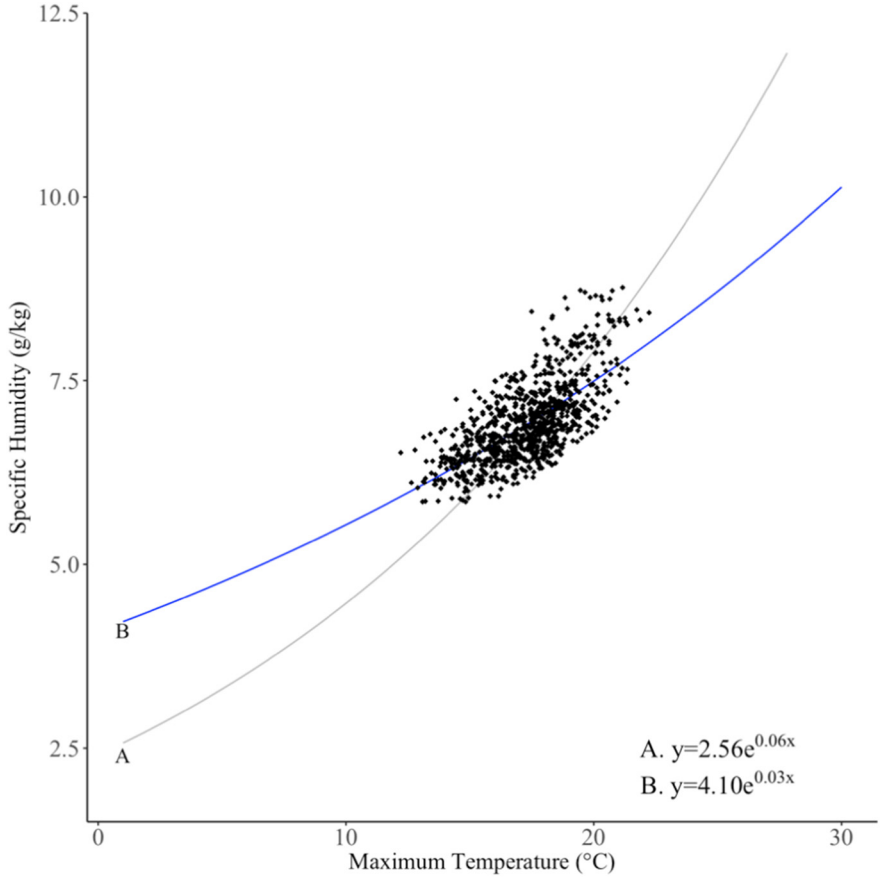

Fig. 4. Exponential relationship between long-term (1982–2012) annual temperature and specific humidity for 31 watersheds located in the central Appalachian Mountains region. The relationship is exponential, following the theoretical Clausius-Clapeyron relationship (Held and Soden, 2006). The relationship states that atmospheric water vapor will exponentially increase with air temperature by 3.4% to 7%/°K (or a slope of $2.45e^{0.06}$) (Held and Soden, 2000), though the observed relationship has a slope ($y = 4.095e^{0.03}$) closer to the lower end of the rates proposed (3.4%/°K) (Allen and Ingram, 2002).

this. SOS in the northeastern United States has increased by 13 days from 1982 to 2012 (0.44 days/year) (Hayhoe et al., 2006; Wolfe et al., 2005), while EOS across the eastern United States has retreated by 12.4 day from 1982 to 2012 (0.4 days/year) (Dragoni and Rahman, 2012). In an earlier study of spring onset in the eastern United States, spring date advanced by 10 days from 1965 to 1980 (Fitzjarrald et al., 2001) and it is likely to continue into the future (see Hayhoe et al. (2006)). Therefore, it is important to understand the exact mechanisms behind changes in growing season length to increase confidence in prediction and modelling to maintain freshwater sustainability in temperate forest watersheds.

5.2. Question 2: what are the predictors of growing season length?

Our results at the landscape level are supported by controlled greenhouse experiments that employed canopy warming methods, which found that air temperatures alone under-predicts observational growing season responses (Wolkovich et al., 2012) and do not explain variations in growing season length due to climate change (Marchin et al., 2015). In general, our results show that a suite of climatic variables that include air temperature, vapor pressure deficit, wind, and humidity explain the greatest amount of variation in growing season length changes in the region. These factors were also shown to be important for vegetation growth in the Qing-Tibetan plateau in China (Hu et al., 2011; Shen et al., 2014). Atmospheric principles can theoretically explain this relationship in which temperatures and changing winds result in higher vapor pressure deficit and evaporative demand (Will et al., 2013; Williams and Baeza, 2007), which subsequently increases atmospheric humidity, a process we collectively refer to as atmospheric water. From these results, we postulate that growing season length responds to temperature and atmospheric water through that Clausius Clapeyron relation, rather than temperature alone. This is consistent with climate chamber experiments which have shown that atmospheric water influences growing season changes via earlier bud burst under constant temperatures (Laube et al., 2014). Furthermore, statistical models with the inclusion of atmospheric water variables explained 27% more of the variation than models with temperature alone (temperature alone = 60% (Liang et al., 2012)), suggesting that there is an interactive effect of temperature and atmospheric humidity on growing season length.

We propose two possible explanations for growing season length responses to atmospheric water and other atmospheric properties: winter dehydration and carbohydrate storage cost/benefit. First, it has been suggested that in aboveground tissues (e.g. xylem), winter dehydration occurs in response to stable low air humidity during cold periods (Laube et al., 2014). Consequently, long cold/dry spells lead to greater dehydration and require higher spring humidity to reach tissue moisture for spring onset (Laube et al., 2014). Trees may detect the onset of growing season through higher minimum temperatures and spring humidity, and the subsequent rehydration of aboveground tissue. Vegetation response to humidity may alleviate the frost damages associated with variable changes in springtime minimum temperatures.

Second, we propose that plants respond to increased availability of resources including humidity, temperature, and solar radiation though a cost/benefit process. The greatest plant carbohydrate storage occurs during direct sunlight, high water content, and nutrient availability (Chapin et al., 1986a). Daily, short term, or seasonal fluctuations alter carbohydrate storage levels (Chapin et al., 1986b), with the lowest

levels occurring during rapid growth and senescence (Chapin, 1977). This is also the point when respiration and growth demands exceed net carbon gains (Nelson and Dickson, 1981). Since plants use carbohydrates acquired during photosynthesis before using stored reserves (Tromp, 1969), senescence represents a point when the cost of using stores needed for spring growth outweighs limited carbon gains from photosynthesis (Estiarte and Peñuelas, 2015). Plants therefore recycle available leaf nutrients back to storage organs (Titus and Kang, 1982). However, a longer growing season with warmer temperatures, direct sunlight, and higher water availability increases the period of net carbon gains, therefore, allowing plants to uptake and store more nutrients for the following (earlier) spring growth period (Chapin III et al., 1990; Keenan and Richardson, 2015; Manzoni et al., 2015).

Current research suggests that leaf out timing is very sensitive to springtime night-length and minimum temperatures (Sakai and Larcher, 2012; Saxe et al., 2001). Our model did not account for the interaction between atmospheric water and minimum temperatures, because our model was developed using annual variables and could not capture the interannual variability. Our study therefore suggests that temperature and humidity work synergistically in annual growing season length changes, although inter-annual variations are likely to be important but beyond the scope of our study. Future research should explore the importance of atmospheric water vapor in identifying inter-annual nuances of green-up and senescence. Current annual prediction models such as the Spring Indices model (Schwartz, 1997), use temperature-based indices and are frequently used throughout the eastern United States (Schwartz, 1997). Hayhoe et al. (2006) used this model to predict growing season length changes throughout the northeast US. Future research should focus on developing a temperature and atmospheric water based index to use in growing season length prediction models (Richardson et al., 2012). Growing season prediction models provides data that allow managers and policy makers to prepare for future changes to watershed sustainability. Future temperature and specific humidity are projected to increase in coming decades (IPCC, 2007), suggesting that single years with unusually high temperature and humidity conditions will potentially result in increasingly unpredictable growing season lengths (e.g. more variability), unreliable forest water cycling/water partitioning, greater long-term ET, and increased occurrences of drought.

5.3. Question 3: does growing season length influence evapotranspiration?

The central Appalachian region is over 80% forested (Slayer, 2014) and returns >40% of P back to the atmosphere as ET. In the southern Appalachia mountains in North Carolina, a one day increase in growing season increased ET by 4.3 mm (Hwang et al., 2014; Hwang et al., 2018; Kim et al., 2018), and in the eastern US, a one day increase in growing season increases ET by 0.2% (or approximately 1 mm/year) (White et al., 1999), as compared to a 0.5 mm increase in our study in central Appalachia. The smaller increase in ET in our study area could be due to reduced water use efficiency, ecosystem dynamics, and land use land cover (LULC) change. First, the effect of increased CO_2 concentration on water use efficiency is outweighed by a longer growing season (Warren et al., 2011). Second, it is also likely that ecosystem dynamics in the semi-dry, energy limited ecosystems do not always represent higher evapotranspiration at all times. Vegetation in these ecosystems has evolved preventative drought stress stomatal dynamics that can decouple the link between increased growing season and evapotranspiration change. Third, forest cover in the study area averages between 60 and 65%, with forests in some areas covering <50% and in other areas almost 100% (Fig. 2). ET increases in the heavily forested areas in sites with high forest cover was likely averaged out with calculating whole watershed scale ET. A one day growing season increase in watersheds that had >65% forest cover averaged around 0.78 mm/one day growing season increase (not shown), suggesting that the agricultural regions reduced ET cycling signals upwards of 0.28 mm/growing season day. Eight watersheds are >30% hay/pasture/agricultural, which is also likely to increase water yield given the occurrences of more intense rainstorms following hydrologic intensification (Huntington and Billmire, 2014). Furthermore, any LULC changes, such as deforestation that has occurred from 1982 to 2012 could mitigate increasing ET signals due to reduced ET cycling in agricultural and urban centers. Therefore, while the lengthened growing season may at least partially influence evapotranspiration trends throughout the central Appalachian region, the intensity of the interaction between growing season and evapotranspiration may vary annually based on water supply conditions. Nevertheless, this analysis gives an indication of a range of potential ET rates (e.g. 0.5 to 4.3 mm) that can occur with a one-day growing season increase in temperate forests.

ET will likely continue to increase in the future, as growing season length continues to increase, having important implications for forested ecosystems that provide clean and stable water to downstream communities. Higher ET has the potential to lead to reduced plant water content, reduced soil moisture, greater incidences of droughts, and decreased long-term water supply to downstream communities. Based on our results, we suggest that scientists implement humidity-based growing season properties such as SOS, EOS, and/or LOS into ET and Q prediction models. Although ET in many large-scale models implicitly reacts to the atmospheric conditions that drive growing season, an explicit representation of humidity based growing season properties could improve the models. The Lund–Potsdam–Jena managed Land (LPJmL) large scale hydrological model (Bondeau et al., 2007), for example, incorporates phenology and other vegetation characteristics allowing for a dynamic growing season representation (Bondeau et al., 2007). However, this may also bring an additional source of uncertainty to Q and ET predictions (Haddeland et al., 2011). Given this assumption, we suggest that models update processing to allow for optional inclusion of phenology and humidity indices, to provide a more accurate prediction of Q and ET for maintaining sustainable forests and freshwater resources.

6. Conclusion and future directions

To understand the role of forests in provisioning water under changing climate, this research determined historical changes in climate, growing season, and ET, investigated the important atmospheric variables effecting growing season length changes, and identified the interaction growing season and evapotranspiration variables. Historical annual growing season length has increased by an average of 22 days while annual ET increased by 12.7 mm across the central Appalachian region of the United States.

Current research suggests that temperature (Dragoni and Rahman, 2012; Morin et al., 2010) and photoperiod alone (Bauerle et al., 2012) are the primary indicators of spring. In general, our results show that multiple climatic variables including temperature, vapor pressure deficit, wind, and humidity are important factors effecting growing season length changes. We postulated that these variables interact synergistically to increase atmospheric water and growing season length through the Clausius-Clapeyron relation. Additionally, over 30 years, a 1.0 day increase in growing season length has generally increased ET by up to 0.5 mm, suggesting that longer growing season may partially influence evapotranspiration trends.

Our research provides important insight into the atmospheric processes responsible for phenology trends and the interaction between climate change induced growing season length and forest ET in eastern US temperate forests. These results will provide important insights for modelling future growing season length and hydrology through the addition of an explicit humidity-based index in current models. The results of this research are likely applicable to temperate forests around the globe that provide potentially valuable information to water resource managers for maintaining watershed sustainability in water-stressed

large global population centers reliant on headwater basins for drinking water and other ecosystem services.

Acknowledgements

Funding for this research was support, in part, by the National Science Foundation Award Number OIA-148952 and the USDA National Institute of Food and Agriculture Hatch project #1004360 awards to Zegre, and the West Virginia University Mountains of Excellence Water Resources STEM Fellowship to Gaertner. Any opinions, findings, and conclusions or recommendations expressed in this material are those of the authors and do not necessary reflect the view of the National Science Found or the USDA. The dataset METDATA was produced by Northwestern University with funding from the NSF Idaho EPScoR Program, the National Science Foundation award number EPS-0814387, and the National Institute for Food and Agriculture competitive grant award 2011-68002-30191.

Appendix A. Supplementary data

Supplementary data to this article can be found online at https://doi.org/10.1016/j.scitotenv.2018.09.129.

References

Abatzoglou, J.T., Brown, T.J., 2012. A comparison of statistical downscaling methods suited for wildfire applications. Int. J. Climatol. 32, 772–780.
Adams, M.B., Edwards, P.J., Ford, W.M., Schuler, T.M., Thomas-Van Gundy, M., Wood, F., 2012. Fernow Experimental Forest: Research History and Opportunities.
Allen, M.R., Ingram, W.J., 2002. Constraints on future changes in climate and the hydrologic cycle. Nature 419, 224–232.
Andreadis, K.M., Lettenmaier, D.P., 2006. Trends in 20th century drought over the continental United States. Geophys. Res. Lett. 33.
ARC, 1970. Subregions in Appalachia. Appalachian Regional Commission.
Arnold, T.W., 2010. Uninformative parameters and model selection using Akaike's information criterion. J. Wildl. Manag. 74, 1175–1178.
Bartoń, K., 2013. MuMIn: multi-model inference. R Package Version 1.9. 13. The Comprehensive R Archive Network (CRAN), Vienna, Austria.
Bauerle, W.L., Oren, R., Way, D.A., Qian, S.S., Stoy, P.C., Thornton, P.E., et al., 2012. Photoperiodic regulation of the seasonal pattern of photosynthetic capacity and the implications for carbon cycling. Proc. Natl. Acad. Sci. 109, 8612–8617.
Bibby, J., Kent, J., Mardia, K., 1979. Multivariate Analysis. Academic Press, London.
Bondeau, A., Smith, P.C., Zaehle, S., Schaphoff, S., Lucht, W., Cramer, W., et al., 2007. Modelling the role of agriculture for the 20th century global terrestrial carbon balance. Glob. Chang. Biol. 13, 679–706.
Breckling, J., 2012. The Analysis of Directional Time Series: Applications to Wind Speed and Direction. Vol. 61. Springer Science & Business Media.
Caldwell, P., Muldoon, C., Ford-Miniat, C., Cohen, E., Krieger, S., Sun, G., et al., 2014. Quantifying the Role of National Forest System Lands in Providing Surface Drinking Water Supply for the Southern United States.
Caldwell, P.V., Miniat, C.F., Elliott, K.J., Swank, W.T., Brantley, S.T., Laseter, S.H., 2016. Declining water yield from forested mountain watersheds in response to climate change and forest mesophication. Glob. Chang. Biol. 22, 2997–3012.
Campbell, J.L., Driscoll, C.T., Pourmokhtarian, A., Hayhoe, K., 2011. Streamflow responses to past and projected future changes in climate at the Hubbard Brook Experimental Forest, New Hampshire, United States. Water Resour. Res. 47, W02514.
Chapin, F.S., 1977. Nutrient/carbon costs associated with tundra adaptations to a cold nutrient-poor environment. Proc. Circumpolar Conference on Northern Ecology. Nat Res Council of Canada, Ottawa, pp. 1183–1194.
Chapin III, F.S., Schulze, E., Mooney, H.A., 1990. The ecology and economics of storage in plants. Annu. Rev. Ecol. Syst. 21, 423–447.
Chapin, F.S., McKendrick, J., Johnson, D., 1986a. Seasonal changes in carbon fractions in Alaskan tundra plants of differing growth form: implications for herbivory. J. Ecol. 707–731.
Chapin, F.S., Shaver, G., Kedrowski, R., 1986b. Environmental controls over carbon, nitrogen and phosphorus fractions in *Eriophorum vaginatum* in Alaskan tussock tundra. J. Ecol. 167–195.
Chmielewski, F.-M., Rötzer, T., 2001. Response of tree phenology to climate change across Europe. Agric. For. Meteorol. 108, 101–112.
Chou, C., Neelin, J.D., Chen, C.-A., Tu, J.-Y., 2009. Evaluating the "rich-get-richer" mechanism in tropical precipitation change under global warming. J. Clim. 22, 1982–2005.
Coopersmith, E., Yaeger, M., Ye, S., Cheng, L., Sivapalan, M., 2012. Exploring the physical controls of regional patterns of flow duration curves–part 3: a catchment classification system based on regime curve indicators. Hydrol. Earth Syst. Sci. 16, 4467–4482.
Creed, I., Hwang, T., Lutz, B., Way, D., 2015. Climate warming causes intensification of the hydrological cycle resulting in changes to the vernal and autumnal windows in a northern temperate forest. Hydrological Processes.
Daly, C., Taylor, G., Gibson, W., 1997. The PRISM approach to mapping precipitation and temperature. Proc., 10th AMS Conf. on Applied Climatology, pp. 20–23.
Daly, C., Halbleib, M., Smith, J.I., Gibson, W.P., Doggett, M.K., Taylor, G.H., et al., 2008. Physiographically sensitive mapping of climatological temperature and precipitation across the conterminous United States. Int. J. Climatol. 28, 2031–2064.
Day, F., Phillips, D., Monk, C., 1988. Forest communities and patterns. Forest Hydrology and Ecology at Coweeta. Springer, pp. 141–149.
Dingman, S.L., 2015. Physical Hydrology. Waveland Press.
Dragoni, D., Rahman, A.F., 2012. Trends in fall phenology across the deciduous forests of the eastern USA. Agric. For. Meteorol. 157, 96–105.
Estiarte, M., Peñuelas, J., 2015. Alteration of the phenology of leaf senescence and fall in winter deciduous species by climate change: effects on nutrient proficiency. Glob. Chang. Biol. 21, 1005–1017.
Farnsworth, R.K., Thompson, E.S., 1983. Mean Monthly, Seasonal, and Annual Pan Evaporation for the United States: US Department of Commerce, National Oceanic and Atmospheric Administration, National Weather Service.
Fernandez, R., Sayama, T., 2015. Hydrological recurrence as a measure for large river basin classification and process understanding. Hydrol. Earth Syst. Sci. 19, 1919–1942.
Fitzjarrald, D.R., Acevedo, O.C., Moore, K.E., 2001. Climatic consequences of leaf presence in the eastern United States. J. Clim. 14, 598–614.
Ford, C.R., Goranson, C.E., Mitchell, R.J., Will, R.E., Teskey, R.O., 2005. Modeling canopy transpiration using time series analysis: a case study illustrating the effect of soil moisture deficit on *Pinus taeda*. Agric. For. Meteorol. 130, 163–175.
Haddeland, I., Clark, D.B., Franssen, W., Ludwig, F., Voß, F., Arnell, N.W., et al., 2011. Multimodel estimate of the global terrestrial water balance: setup and first results. J. Hydrometeorol. 12, 869–884.
Harstine, L.J., 1991. Hydrologic Atlas for Ohio: Average Annual Precipitation, Temperature, Streamflow, and Water Loss for 50-year Period, 1931–1980. Ohio Department of Natural Resources, Division of Water, Ground Water Resources Section.
Hayhoe, K., Wake, C.P., Huntington, T.G., Luo, L., Schwartz, M.D., Sheffield, J., et al., 2006. Past and future changes in climate and hydrological indicators in the US northeast. Clim. Dyn. 28, 381–407.
Held, I.M., Soden, B.J., 2000. Water vapor feedback and global warming. Annu. Rev. Energy Environ. 25, 441–475.
Held, I.M., Soden, B.J., 2006. Robust responses of the hydrological cycle to global warming. J. Clim. 19, 5686–5699.
Helsel, D.R., Hirsch, R.M., 1992. Statistical Methods in Water Resources. Elsevier, Amsterdam.
Hirsch, R.M., De Cicco, L.A., 2015. User Guide to Exploration and Graphics for RivEr Trends (EGRET) and dataRetrieval: R Packages for Hydrologic Data. US Geological Survey.
Hirsch, R.M., Slack, J.R., 1984. A nonparametric trend test for seasonal data with serial dependence. Water Resour. Res. 20, 727–732.
Homer, C., Dewitz, J., Yang, L., Jin, S., Danielson, P., Xian, G., et al., 2015. Completion of the 2011 National Land Cover Database for the conterminous United States–representing a decade of land cover change information. Photogramm. Eng. Remote. Sens. 81, 345–354.
Hong, G., Zhang, Y., 2006. Object-based change detection in high resolution image. In: Sensing ASfPaR (Ed.), Proceedings of the ASPRS 2006 Annual Conference, Reno, Nevada.
Hu, M.Q., Mao, F., Sun, H., Hou, Y.Y., 2011. Study of normalized difference vegetation index variation and its correlation with climate factors in the three-river-source region. Int. J. Appl. Earth Obs. Geoinf. 13, 24–33.
Huntington, T.G., 2010. Climate warming-induced intensification of the hydrologic cycle. Adv. Agron. 109, 1–53.
Huntington, T.G., Billmire, M., 2014. Trends in precipitation, runoff, and evapotranspiration for rivers draining to the Gulf of Maine in the United States. J. Hydrometeorol. 15, 726–743.
Hwang, T., Band, L.E., Miniat, C.F., Song, C., Bolstad, P.V., Vose, J.M., et al., 2014. Divergent phenological response to hydroclimate variability in forested mountain watersheds. Glob. Chang. Biol. 20, 2580–2595.
Hwang, T., Martin, K.L., Vose, J.M., Wear, D., Miles, B., Kim, Y., et al., 2018. Non-stationary hydrologic behavior in forested watersheds is mediated by climate-induced changes in growing season length and subsequent vegetation growth. Water Resources Research.
IPCC, 2007. The physical science basis. Contribution of WG1 to the Fourth Assessment Report of the Intergovernmental Panel on Climate Change, 2007.
Jeong, S.-J., Ho, C.H., Gim, H.J., Brown, M.E., 2011. Phenology shifts at start vs. end of growing season in temperate vegetation over the Northern Hemisphere for the period 1982–2008. Glob. Chang. Biol. 17, 2385–2399.
Jones, J.A., Creed, I.F., Hatcher, K.L., Warren, R.J., Adams, M.B., Benson, M.H., et al., 2012. Ecosystem processes and human influences regulate streamflow response to climate change at long-term ecological research sites. Bioscience 62, 390–404.
Jönsson, P., Eklundh, L., 2004. TIMESAT—a program for analyzing time-series of satellite sensor data. Comput. Geosci. 30, 833–845.
Keenan, T.F., Richardson, A.D., 2015. The timing of autumn senescence is affected by the timing of spring phenology: implications for predictive models. Glob. Chang. Biol. 21, 2634–2641.
Keim, B.D., 1996. Spatial, synoptic, and seasonal patterns of heavy rainfall in the southeastern United States. Phys. Geogr. 17, 313–328.
Keim, B.D., 1997. Preliminary analysis of the temporal patterns of heavy rainfall across the southeastern United States. Prof. Geogr. 49, 94–104.
Kim, J.H., Hwang, T., Yang, Y., Schaaf, C.L., Boose, E., Munger, J.W., 2018. Warming-induced earlier greenup leads to reduced stream discharge in a temperate mixed forest catchment. J. Geophys. Res. Biogeosci. https://doi.org/10.1029/2018JG004438.
Konrad, C.E., Fuhrmann, C.M., 2013. Climate of the southeast USA: past, present, and future. Climate of the Southeast United States. Springer, pp. 8–42.

Koster, R.D., Suarez, M.J., 1999. A simple framework for examining the interannual variability of land surface moisture fluxes. J. Clim. 12, 1911–1917.
Laube, J., Sparks, T.H., Estrella, N., Menzel, A., 2014. Does humidity trigger tree phenology? Proposal for an air humidity based framework for bud development in spring. New Phytol. 202, 350–355.
Lebourgeois, F., Pierrat, J.-C., Perez, V., Piedallu, C., Cecchini, S., Ulrich, E., 2010. Simulating phenological shifts in French temperate forests under two climatic change scenarios and four driving global circulation models. Int. J. Biometeorol. 54, 563–581.
Liang, L., Schwartz, M.D., Fei, S., 2012. Photographic assessment of temperate forest understory phenology in relation to springtime meteorological drivers. Int. J. Biometeorol. 56, 343–355.
Manzoni, S., Vico, G., Thompson, S., Beyer, F., Weih, M., 2015. Contrasting leaf phenological strategies optimize carbon gain under droughts of different duration. Adv. Water Resour. 84, 37–51.
Marchin, R.M., Salk, C.F., Hoffmann, W.A., Dunn, R.R., 2015. Temperature alone does not explain phenological variation of diverse temperate plants under experimental warming. Glob. Chang. Biol. 21, 3138–3151.
McCune, B., Grace, J.B., Urban, D.L., 2002. Analysis of Ecological Communities. Vol. 28. MjM software design Gleneden Beach, OR.
Miller, M., Weaver, C., 1971. Snow in Ohio. Ohio Agricultural Research and Development Center. Research Bulletin. 1044.
Morin, X., Roy, J., Sonié, L., Chuine, I., 2010. Changes in leaf phenology of three European oak species in response to experimental climate change. New Phytol. 186, 900–910.
Nelson, E.A., Dickson, R.E., 1981. Accumulation of food reserves in cottonwood stems during dormancy induction. Can. J. For. Res. 11, 145–154.
Parker, H.N., Willis, B., Bolster, R., Ashe, W., Marsh, M., 1907. The Potomac River basin. Water Supply Irrig. Pap. 192, 297.
Patterson, L.A., Lutz, B., Doyle, M.W., 2012. Streamflow changes in the South Atlantic, United States during the mid- and late 20th Century. J. Am. Water Res. Assoc. 48, 1126–1138.
Penman, H.L., 1948. Natural evaporation from open water, bare soil and grass. Proceedings of the Royal Society of London A: Mathematical, Physical and Engineering Sciences. 193. The Royal Society, pp. 120–145.
Pinzon, J.E., Tucker, C.J., 2014. A non-stationary 1981–2012 AVHRR NDVI3g time series. Remote Sens. 6, 6929–6960.
Pitchford, J., Wu, C., Lin, L., Petty, J., Thomas, R., Veselka, W., et al., 2011. Climate change effects on hydrology and ecology of wetlands in the mid-Atlantic highlands. Wetlands 1–13.
Prebyl, T.J., 2012. An Analysis of the Patterns and Processes Associated With Spring Forest Phenology in a Southern Appalachian Landscape Using Remote Sensing. UGA.
Ratner, B., 2009. The correlation coefficient: its values range between +1/−1, or do they? J. Target. Meas. Anal. Mark. 17, 139–142.
RCore, 2013. R: A Language and Environment for Statistical Computing.
RCore, 2014. R: A Language and Environment for Statistical Computing. R Foundation for Statistical Computing, Vienna, Austria 3-900051-07-0.
Richardson, A.D., Bailey, A.S., Denny, E.G., Martin, C.W., O'keefe, J., 2006. Phenology of a northern hardwood forest canopy. Glob. Chang. Biol. 12, 1174–1188.
Richardson, A.D., Anderson, R.S., Arain, M.A., Barr, A.G., Bohrer, G., Chen, G., et al., 2012. Terrestrial biosphere models need better representation of vegetation phenology: results from the North American Carbon Program Site Synthesis. Glob. Chang. Biol. 18, 566–584.
Sakai, A., Larcher, W., 2012. Frost Survival of Plants: Responses and Adaptation to Freezing Stress. Vol. 62. Springer Science & Business Media.
Sankarasubramanian, A., Vogel, R.M., 2002. Annual hydroclimatology of the United States. Water Resour. Res. 38.
Saxe, H., Cannell, M.G., Johnsen, Ø., Ryan, M.G., Vourlitis, G., 2001. Tree and forest functioning in response to global warming. New Phytol. 149, 369–399.
Schwartz, M.D., 1997. Spring index models: an approach to connecting satellite and surface phenology. Phenology in Seasonal Climates I, pp. 23–38.
Schwartz, M.D., Reed, B.C., White, M.A., 2002. Assessing satellite-derived start-of-season measures in the conterminous USA. Int. J. Climatol. 22, 1793–1805.
Schwartz, M.D., Ahas, R., Aasa, A., 2006. Onset of spring starting earlier across the Northern Hemisphere. Glob. Chang. Biol. 12, 343–351.
Shen, Z., Fu, G., Yu, C., Sun, W., Zhang, X., 2014. Relationship between the growing season maximum enhanced vegetation index and climatic factors on the Tibetan Plateau. Remote Sens. 6, 6765–6789.
Slack, J.R., Landwehr, J.M., 1992. Hydro-climatic Data Network (HCDN); a US Geological Survey Streamflow Data Set for the United States for the Study of Climate Variations, 1874–1988. US Geological Survey (Copies of this report can be purchased from USGS Books and Open-File Reports Section).
Slayer, K.L., 2014. Central Appalachians: Ecoregion Description. United States Geologic Survey.
Titus, J.S., Kang, S.M., 1982. Nitrogen metabolism, translocation, and recycling in apple trees. Hortic. Rev. 4, 204–246.
Trenberth, K.E., Smith, L., Qian, T., Dai, A., Fasullo, J., 2007. Estimates of the global water budget and its annual cycle using observational and model data. J. Hydrometeorol. 8, 758–769.
Troch, P.A., Martinez, G.F., Pauwels, V.R., Durcik, M., Sivapalan, M., Harman, C., et al., 2009. Climate and vegetation water use efficiency at catchment scales. Hydrol. Process. 23, 2409–2414.
Tromp, J., 1969. Storage and mobilization of nitrogenous compounds in apple trees with special reference to arginine. Long Ashton Symp, 2d. Univ of Bristol.
U.S._Census_Bureau, 2009. National population estimates: characteristics. http://www.census.gov/popest/national/asrh/NC-EST2005-asrh.html.
Vidal, M., Amigo, J.M., 2012. Pre-processing of hyperspectral images. Essential steps before image analysis. Chemom. Intell. Lab. Syst. 117, 138–148.
Viviroli, D., Weingartner, R., 2004. The hydrological significance of mountains: from regional to global scale. Hydrol. Earth Syst. Sci. Discuss. 8, 1017–1030.
Viviroli, D., Dürr, H.H., Messerli, B., Meybeck, M., Weingartner, R., 2007. Mountains of the world, water towers for humanity: typology, mapping, and global significance. Water Resour. Res. 43.
Wang, D., Hejazi, M., 2011. Quantifying the relative contribution of the climate and direct human impacts on mean annual streamflow in the contiguous United States. Water Resour. Res. 47.
Warren, J.M., Pötzelsberger, E., Wullschleger, S.D., Thornton, P.E., Hasenauer, H., Norby, R.J., 2011. Ecohydrologic impact of reduced stomatal conductance in forests exposed to elevated CO_2. Ecohydrology 4, 196–210.
White, M., Running, S., Thornton, P., 1999. The impact of growing-season length variability on carbon assimilation and evapotranspiration over 88 years in the eastern US deciduous forest. Int. J. Biometeorol. 42, 139–145.
White, M.A., Beurs, D., Kirsten, M., Didan, K., Inouye, D.W., Richardson, A.D., et al., 2009. Intercomparison, interpretation, and assessment of spring phenology in North America estimated from remote sensing for 1982–2006. Glob. Chang. Biol. 15, 2335–2359.
Will, R.E., Wilson, S.M., Zou, C.B., Hennessey, T.C., 2013. Increased vapor pressure deficit due to higher temperature leads to greater transpiration and faster mortality during drought for tree seedlings common to the forest–grassland ecotone. New Phytol. 200, 366–374.
Williams, L.E., Baeza, P., 2007. Relationships among ambient temperature and vapor pressure deficit and leaf and stem water potentials of fully irrigated, field-grown grapevines. Am. J. Enol. Vitic. 58, 173–181.
Wolfe, D.W., Schwartz, M.D., Lakso, A.N., Otsuki, Y., Pool, R.M., Shaulis, N.J., 2005. Climate change and shifts in spring phenology of three horticultural woody perennials in northeastern USA. Int. J. Biometeorol. 49, 303–309.
Wolkovich, E.M., Cook, B.I., Allen, J.M., Crimmins, T.M., Betancourt, J.L., Travers, S.E., et al., 2012. Warming experiments underpredict plant phenological responses to climate change. Nature 485, 494.
Yue, S., Pilon, P., Cavadias, G., 2002. Power of the Mann–Kendall and Spearman's rho tests for detecting monotonic trends in hydrological series. J. Hydrol. 259, 254–271.
Zegre, N.P., Miller, A.J., Maxwell, A., Lamont, S.J., 2014. Multiscale analysis of hydrology in a mountaintop mine-impacted watershed. J. Am. Water Res. Assoc. 50, 1257–1272.
Zuur, A., Ieno, E., Walker, N., Saveliev, A., Smith, G., 2009. In: Gail, M., Krickeberg, K., Samet, J.M., Tsiatis, A., Wong, W. (Eds.), Mixed Effects Models and extensions in Ecology With R. Spring Science and Business Media, New York, NY.